Development and performance evaluation of instrumented subsoilers in breaking soil hard-pan

Odey Simon Ogbeche[1*], Manuwa Seth Idowu[2], Ewetumo Theophilus[3]

(1. *Department of Wood Products Engineering, Cross River University of Technology, Calabar, Nigeria*;

2. *Department of Agricultural and Environmental Engineering, The Federal University of Technology, Akure, Nigeria*;

3. *Department of Physics, The Federal University of Technology, Akure, Nigeria*)

Abstract: Four instrumented subsoilers were developed for alleviation of compaction on agricultural land. Draughts and soil disturbance of the subsoilers were measured during operation at the outdoor soil bin. Straight shank subsoiler (SSS), Straight shank subsoiler at 37° rake angle (SSS37), semi-parabolic subsoiler (SPS), parabolic 'C' shank subsoiler (CSS) and winged subsoiler (WSB) were designed and constructed for use by the tool carrier in loosening soil hard pan. Soil cone penetrometer (CP40II, 333 mm^3, 60° cone tip angle) and electronic moisture meter were used to take readings at various locations and depths on the soil bin before and after subsoiling. Soil samples were taken to laboratory for analysis for physico-chemical properties. Each of the shanks was hitched to the tool bar of the carrier. A 100 kN calibrated load cell was connected to the tool carrier via the drawbar of a 31.6 kW (MF 415) Massey Fergusson tractor. The load cell was connected to the data logger via instrumentation amplifier. Laptop computer system was connected to the data *logger* to download the draught data for each shank which was operated at four levels of depth –20, 30, 40 and 50 cm. Profilometer of dimension 80 by 75 cm height and width respectively was used to measure the area of soil disturbance by each subsoiler. Data collected were analyzed to establish relevant relationships between subsoiler draughts and tillage parameters in the form of correlation, regression models and graphs. Results showed that the best subsoiler in terms of draught reduction was parabolic C-shank subsoiler (CSS) with 4.581 kN, followed by semi-parabolic subsoiler (SPS) with draught of 4.905 kN at depth of 40 cm. At this working depth the SSS, WSB and SSS37 had draughts of 6.874, 7.003 and 7.385 kN respectively. Thus, WSB had the highest power requirement followed by straight shank subsoiler at 37° rake angle (SSS37), both had 34.09 and 31.20 kW at 50 cm depth respectively. Thus at 20 cm depth of operation WSB and SSS37 subsoilers had 13.95 and 14.29 kW respectively. CSS had the lowest power requirement followed by SPS with 5.55 and 7.76 kW respectively. Straight shank subsoiler at 37° rake angle, SSS37 showed the highest soil loosening ability at all the depths followed by WSB, SPS, SSS and CSS respectively. Thus, at 50 cm highest working depth SSS had 0.0451 m^2 followed by SPS with 0.0487 m^2, while CSS, WSB and SSS37 had 0.0403, 0.0683 and 0.1061 m^2 respectively. Regression equations were established for the draught of each subsoiler. They all had R^2 of more than 99%. Draught of subsoilers had high positive correlation with depth, cone index (CI) and bulk density (BD), and negative correlation with soil moisture (MC) and porosity (PR).

Keywords: subsoilers, depth, draughts, power requirements, soil disturbance, hard-pan, cone index

1 Introduction

Subsoilers have been of great benefits in the alleviation of soil compaction. Their applications in breaking soil hard pan layer, especially on agricultural soils have been a great relief to farmers in developed countries of the world. Developing countries however, have not keyed into this important operation in appropriate agricultural mechanization; as most farmers keep tilling their land year-in-year-out using ploughs and harrows which cannot pulverise the soil to depth of 35 cm and above where soil hard-pan exists on most agricultural soils. Many soils around the globe have a hard-pan at about 15 to 36 cm deep and 5 to 15 cm thick (Radcliffe *et al.*, 1989; Taylor, 1990; Clark et al, 2000; Kumar and

Thakur, 2005). To alleviate the problems of soil compaction, subsoiling is carried out. Subsoiling or deep tillage is a field operation usually performed using a subsoiler to break up compacted layers of soil at depths of 25-90 cm and 60-150 cm space channels without inversion, using knife-like shanks that are pulled through the soil to create continuous grooves. The subsoiler is similar in principle to the chisel, but it is more heavily built and rigid for operation at depths of up to 90 cm to loosen deep soil layers for the promotion of water movement through the tillage pan, and to enhance soil conservation, soil moisture storage, root growth, and crop yields (Raper *et al.*, 1998; Abu-Hamdeh, 2003; Williams *et al.*, 2006).

There exist different shapes of shank designs in subsoiler. Shank design affects subsoiler performance, shank strength, surface and residue disturbance, effectiveness in fracturing soil, and the horsepower required to pull the subsoiler (Sakai *et al.*, 1993; Godwin, 2007; Kees, 2008). Such shapes are Swept shank, Straight shank, Curved (semi-parabolic) shank, Parabolic shank, Winged type and no-wing type, rotary, Vibration and non-vibration types, Coulter subsoiler, Coulter with blades subsoiler, Coulter with blades and reversing subsoiler. Thus, subsoilers are designed with various shapes depending on the form of subsoiling operation that will be performed. An important consideration concerning subsoiling is the amount of soil disruption for different soil conditions to increase the long-term benefits of subsoiling (Raper and Sharma, 2004). Celik and Raper (2012) reported that many subsoilers have been designed and tested, using a number of subsoiling techniques for alleviating compacted layers of various types and conditions of soils.

Plants grown in compacted soils have shown a smaller number of lateral roots than plants grown under controlled condition. Plants grown in more compacted soils showed smaller ratios of fresh to dry mass. Soil compaction have adverse effect upon crops by – increasing the mechanical impedance to the growth of roots; altering the extent and configuration of the pore space and aggravating root diseases (Tardieu, 1994; Amauri *et al.*, 2008; Isaac *et al.*, 2002; Borghei *et al.*, 2008; Weber and Biskupski, 2008; Soltanabadi *et al.*,

2008; Grzesiak, 2009; Juliano and Rosolem, 2010; Kulkarni *et al.*, 2010; Becerra and Botta *et al.*, 2010; Becerra and Tourn, 2011; Chen and Weil, 2011; Otto *et al.*, 2011).

As recorded by Mason *et al.* (1988) that the ability of plant roots to penetrate soil is restricted as soil strength increases and ceases entirely at 2.5 MPa. Increase in cone index of soil has been found to restrict growth of crop roots (Atwell, 1993; Gregory, 1994). Thus, an inverse relationship exists between cone index and crop roots (Bengough, 1991; Atwell, 1993). Aase *et al.* (2001) reported that as cone index approached 2. 0 MPa and moved above this value, root growth had been restricted to varying degrees. Hence, 2.0 MPa has been considered as a measure in the determination of soil hard pan layer (Wells *et al.*, 2005). Raper *et al.* (1998) further revealed that critical limit of penetration resistance restraining root distribution was within 40-50 cm soil depth and that subsoiling could reduce and provide increased rooting depth. Some outstanding results have been achieved from subsoiling. Yield increase of 50 to 400 percent has been reported from subsoiling under the right soil and moisture conditions and in the right areas (Borghei *et al.*, 2008).

Measurement of forces on tillage tools have been an issue of great concern in soil tillage dynamics. Draught measurements are required for many studies including energy input for field equipment, matching tractor to an implement size, and tractive performance of a tractor. Vertical force affects weight transfer from implement to the tractor, and consequently, affects the tractive performance and dynamic stability of the tractor (Chen *et al.*, 2007). Many researchers have used various devises to measure draught of tillage tools: Manor and Clark (2001), Manuwa (2002), Al-Suhaibani *et al.* (2010) and Ademosun (2014) reported different types of instrumentations such as transducer, dynamometer, strain gauge, extended orthogonal ring transducer and the use of load cell, utilized in the measurement of forces on tillage tools. Thus, the objectives of this work are:

a) To design and develop subsoilers for alleviation of compaction on agricultural land;

b) To design, fabricate components and assemble electronic instrumentation for the acquisition and logging of draught data; and

c) To evaluate the performance of the subsoilers.

2   Materials and methods

2.1   Experimental site

The experiment was carried out on the outdoor soil bin facility at the Science and Technology Education Post-Basic (STEP-B) Research Field of the Federal University of Technology, FUTA, Akure; located on geographical coordinate, 7°15′0″N and 5°11′42″E. The study was conducted in the 2015/2016 academic session.

2.2   Experimental procedure

The experimental procedure is elaborated below.

2.2.1   Design of subsoiler shanks

Design of subsoiler shanks was carried out according to Ashrafizadeh and Kushwaha (2003), Godwin (2007), Aikins and Kilgour (2007), Mollazade *et al.* (2010), Odey and Manuwa (2016), where a step-by-step approach was followed in the design of narrow tillage tools. Firstly, parameters such as angle of shearing resistance, $\phi = 22°$, angle of soil metal friction, $\delta = 10°$, soil cohesion, $C = 5.2$ kN m^{-2}, bulk unit weight of soil, $\gamma = 17.4$ kN m^{-3} and adhesion, $Ca = 2.6$ kN m^{-2}, were chosen. Rake angles which vary from 16° to 58° (inclined tine) in previous works (Rahman *et al.*, 2001) were also chosen.

Determination of other parameters were carried out. These include subsoiler width (m), angle between the tine face and the soil failure plane at working depth (Θ), critical rake angle (αc), tine inclination factor (K), tine category, sectional area of soil loosened behind a tine, void (v) created by the Shank, soil shear plane angle (β) in degree, side crescent (s), maximum crescent angle (ℓ), N-factors, total tool force on shank (F), forward failure force (Ff), sideways failure force (Fs), draught force (H), vertical force (V), resultant force acting on shank (RF), bending moment on the shank (Mb), thickness of the shank blade (t) and determination of power requirement to pull the shank (P) (Odey and Manuwa, 2016).

2.2.2   Fabrication of subsoilers

Fabrication of components were carried out in Agricultural Engineering Workshop, Federal University of Technology, FUTA. The subsoiler shoes were cut from 60 mm×60 mm medium carbon steel bar using the oxyacetylene flame cutter into their respective sizes, and thereafter machined. Holes were drilled accordingly using vertical drilling machine (using appropriate drill britt) on the shoes for coupling of parts such as subsoiler blade and wings.

Subsoiler blades were cut to size using electric hand cutting machine to 60 mm width, 230 mm length and 150 mm thickness. Two of such blades were adapted for use with all the shanks. The subsoiler shanks were cut using oxyacetylene flame cutter to their respective sizes from a medium carbon steel plate of 20 mm diameter. Each of the shanks was welded accordingly to the shoe using electric arc welding machine with stainless electrodes.

A medium carbon steel bar of 55 mm×55 mm× 1,000 mm was cut using the flame cutter. A slot 24 mm wide and 100 mm deep was created on one side of the tool bar for the purpose of attaching each of the shanks. Three holes of 18 mm diameter were drilled 30 mm apart for bolting each shank firmly to the tool bar.

2.2.3   Description of Subsoiler Shanks

The subsoiler shanks developed are shown in Figure 1 and 4 as described below.

(a) Straight Shank Subsoiler (SSS)

Straight shank subsoiler (SSS) had a total height of 600 mm, thickness of 20 mm and width of 60 mm. It had a shoe of length 300 mm, with a cutting blade of length 230 mm and thickness of 150 mm. It has a lift cutting angle (rake angle) of 27°, as recommended by Sakai *et al.* (1983) and used by Bandalan *et al.* (1999); and Kumar and Tharkur (2005). The shoe had two holes located 40 mm apart on the sides for the attachment of wings using bolts. The shoe also had two holes drilled 70 mm apart for bolting the cutting blade. The cutting blade can easily be attached to the shoe with the use of bolts and nuts and was replaceable.

(b) Winged subsoiler (WSB)

When two wings of 70 mm wide each were attached at opposite sides of the shoe, the result was winged subsoiler.

(c) Semi-parabolic subsoiler (SPS)

This shank had a height of 600 mm, and was slightly curved towards the shoe, with its contact at the heel. The shoe had a length of 180 mm.

(d) Parabolic 'C' shank subsoiler (CSS)

This was completely curved, and had a "C" shape. It

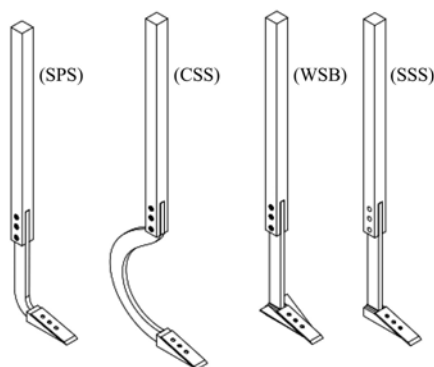had a height of 600 mm, thickness of 20 mm and width of 60 mm.

Figure 1   Subsoiler shanks attached to the tool bar: Semi-parabolic (SPS), Parabolic 'C' shank (CSS), Winged (WSB), and Straight shank subsoilers (SSS)

2.3   Description of the soil bin and its facilities

2.3.1   Soil bin

Ale *et al.* (2013) reported that the soil bin facility was equipped with a soil bin with a dimension of 48,000× 1500×1200 mm of length, width and height, respectively. The walls of the soil bin were constructed with concrete blocks. The blocks were clad with bin wall panels for better reinforcement, rigidity, and efficient and effective behaviour of bin walls in service. The bin wall panel was fabricated from mild steel plate 8 mm thick, inverted L-section 150×1050×2400 mm, with drilled holes for installation.

Two steel rails run parallel to each other along the whole length of the bin. They are made from steel angle sections 150×150×10 mm and installed on concrete shoulder of the bin by means of drilled holes (on the railings) 12 mm diameter countersunk at 60 degrees at 1,000 mm intervals. The implement carriage was designed to run on the railings which horizontal surface width was compatible with the running wheels of the implement carriage.

2.3.2   Implement carriage system

The implement carriage was constructed using rectangular hollow section steel (RHS) of dimension 100×100 mm and is supported on four wheels mounted on the main frame by four-wheel mounting brackets. The arrangement of the wheels was designed to run on the side railings of the soil bin. The carriage has a three-point linkage and also has an implement coupling recess to enhance the rigid coupling of the tool carriage sub system.

The carriage dimension is 1,623 mm×700 mm× 1,117 mm of length, width and height, respectively. The major functions of the carriage are: 1) to mount the carriage subsystem which in turn carries the toolbar in place; and 2) to mount any tillage or traction devices such as traction or towed wheels for testing or for transportation. The carriage can be coupled to the power source through the 3-point linkage, and by using the bracket system through the drawbar.

2.3.3   Implement carriage sub-system

This is basically made up of a rectangular main frame designed to stand on four detachable steel legs. The middle of the frame is welded of a rake meter for varying the angle of approach (rake angle) of mounted tool or implement. Also, it is a mounting device to hold the tool bar rigidly in place at that point below the rake meter. The carriage subsystem has dimension of 1,395 mm× 600 mm×667 mm of length, width and height, respectively. Two mounting studs are also welded in place to secure rigidity with the implement carriage.

2.3.4   Soil levelling blade

The levelling blade consisted essentially of a plane steel board with light curvature, 1400 mm wide and 350 mm height. It was reinforced at the middle to provide sufficient strength and rigidity. Provision was made by means of slot-pinning device to attach it to the tool bar.

2.3.5   Smooth compaction roller

The soil compaction roller consisted mainly of a cylindrical drum, the roller axle and bearing and ballast weights. The diameter and length of the roller drum were 700 and 1,350 mm, respectively. The coupling frame width and length were 1,700 and 400 mm, respectively. The weight of the roller without the ballast weights was 85 kg. Ten weights each of 5 kg were provided for ballasting. The axle of the compaction roller was supported in two bearing housing. Provision was made for the roller to be moved in the vertical direction or be suspended in space through the position adjustment device. The vertical adjustment was accomplished by raising or lowering the roller through the vertical adjustment. The roller was designed to be coupled to the implement carriage and its major function is to compact the bin soil in layers as desired for testing.

2.3.6 Spiked roller

The spiked roller is similar to the smooth roller and has the same dimension. However, it has spikes welded to the surface along the periphery. The spikes are of length 20 mm and diameter 20 mm. The function of the spiked roller was to ensure a satisfactory bond between successive soil layers.

2.3.7 Tool bar and fixing device (modification)

The tool bar was fabricated from 55 mm square section solid bar (medium carbon steel) of length 1000 mm. A slot 24 mm wide and 100 mm deep was created on one side of the tool bar for the purpose of hitching each of the shanks. Three holes of 18 mm diameter were drilled 30 mm apart for bolting each shank firmly to the tool bar. The existing tool bar which had

tool bar clamp devices for tool/ implement coupling was replaced with the tool bar having a slot for easy attachment of shank. This served as a modification to the existing one (see Figures 2 and 3 below).
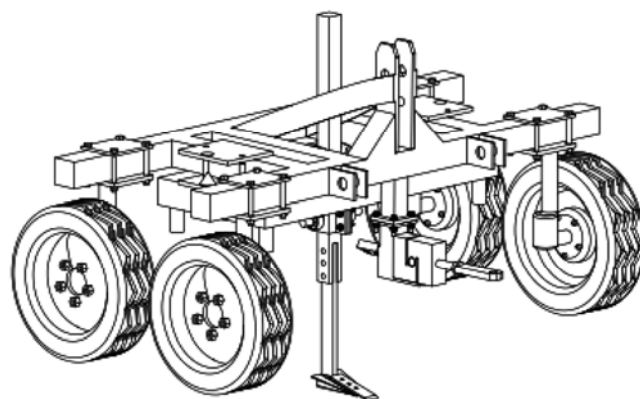
Figure 2   Winged subsoiler attached to the tool carrier via the tool bar
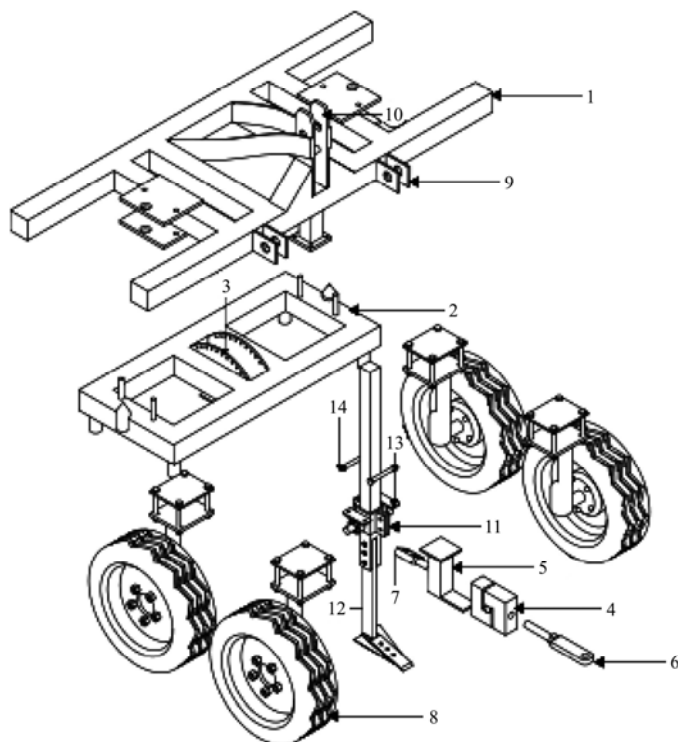
Figure 3   Exploded view of the tool carrier with winged subsoiler and load cell attached

Part list		
S/N	Discription	QTY
1	Implement carriage	1
2	Implement carriage sub-system	1
3	Rake meter	1
4	Load cell	1
5	Load cell seat	1
6	Load cell bracket (front)	1
7	Load cell bracket (back)	1
8	Implement carriage wheel	4
9	Lower link attachment	2
10	Upper link attachment	1
11	Tool bar holder	1
12	Tool bar	1
13	Bearing	1
14	Bolt and nut	30

2.3.8 Instrumentation assembly

The instrumentation system consists of the follows: (a) Load cell (100 kN) – strain gauge type (No. 100201022 and output, 2.50mV V^{-1}), (b) Load cell bracket, (c) Load cell amplifier board (print circuit board), (d) Data logger – Grant – SQ2040/2F16 and (e) HP Laptop computer system. The data logger is equipped with software, SquirelView Plus edition, version 5.3.6. The software has the ability to download logged data from the logger into the computer. In other to view the data, it must be

converted by SquirrelView for Analysis or exported to excel (.xls) format.

2.4 Soil test

The soil bin and its environs were cleared and packed. The soil bin was mapped out and divided into four zones of length, 12,000 mm each, for study. The zones were captioned A, B, C, and D.

2.4.1 Soil bulk density:

Soil samples were taken from each of the zones on the soil bin at 3 depths of 0-15, 16-30, 31-45 cm using soil

core samplers for measurement of soil bulk density. Soil cores were driven into each depth of the soil and the collected soil was kept in an air tight polythene bag to avoid moisture loss. The samples were oven dried and weighted. The oven dried soil in the cores were allowed to cool. The bulk density was determined using equation (Blake and Hartge, 1986; D'Haene *et al.*, 2008).

2.4.2   Moisture content

Moisture meter (model – PMS – 714) was used to take soil moisture content in-situ at specific zones on the soil bin.

2.4.3   Soil porosity

Direct method was used in measuring the porosity. Firstly, the bulk volume of the porous sample was determined, then the volume of the skeletal material with no pores was determined. Thus, pore volume = total volume − material volume. This was done for each of the samples according to Blake and Hartge, (1986), D'Haene *et al.* (2008).

2.4.4   Cone index

In other to ascertain the degree of compaction of the soil on each zone of the soil bin, cone index was measured to be 50 cm of depth by using cone penetrometer (model - CP40II, RIMIK, Australia). The penetrometer is equipped with load cell, transducer, GPS and LCD screen.

2.5   Compaction of soil in the bin

The subsoiler shanks were designed to break hard pans of soil to a depth of 500 mm. Hard pans of 2.0 MPa and above is highly detrimental to crop production. Therefore, there was the need to re-compact the soil after loosening with each of the subsoiler. The tractor was carefully driven to and fro along the soil bin with two wheels (front and back) in and two wheels (front and back) out of the soil bin. By doing this, the soil was easily recompacted due to the immense weight of the tractor on it (Celik and Raper, 2012). The rollers were not found suitable for this purpose due to their low weight (85 kg) compared to that of the tractor (2,018 kg). After each re-compaction the cone index was measured to ensure a surface and sub-soil compaction of at least 2.0 MPa and above.

2.6   Experimental design

The compacted soil bin of length, 48,000 mm was

divided into six with a distance of 8,000 mm apart for testing of each of the developed subsoilers. Five soil profiles (400 mm by 700 mm and 550 mm deep) were dug 8,000 mm apart through the length of the soil bin for testing each of the subsoilers. This was done in other to facilitate the mounting and adjustment of the depth of operation of the subsoiler on the tool bar. Thus, the soil bin was re-compacted after the operation of each of the subsoilers on the replicated soil profiles (see Figure 4 and 5).
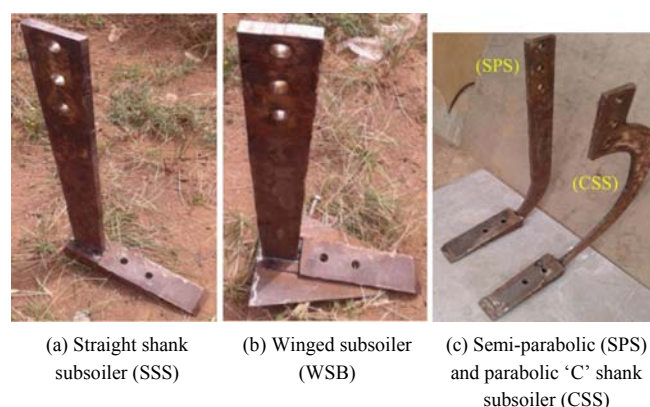

(a) Straight shank subsoiler (SSS)   (b) Winged subsoiler (WSB)   (c) Semi-parabolic (SPS) and parabolic 'C' shank subsoiler (CSS)

Figure 4   Showing fabricated different subsoilers

(a) Straight shank and load cell in position   (b) Semi-parabolic and load cell in position

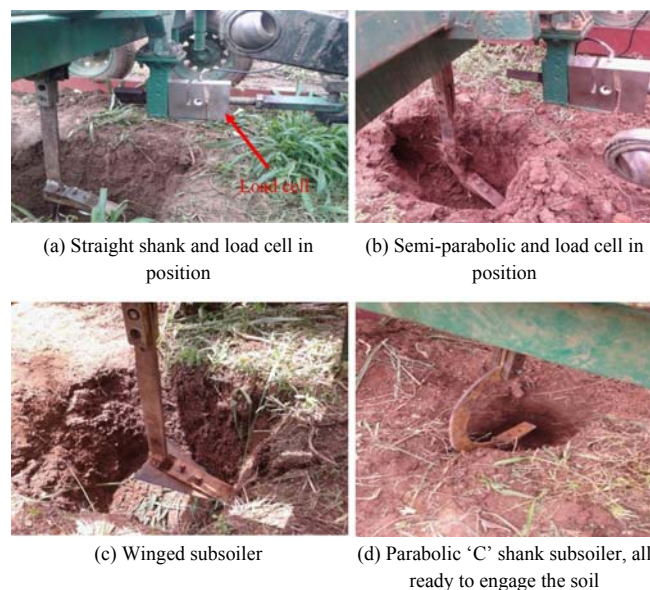(c) Winged subsoiler   (d) Parabolic 'C' shank subsoiler, all ready to engage the soil

Figure 5   Showing different subsoilers in ready to engage the soil

2.7   Testing of subsoilers

This experiment took a total of four weeks, beginning from 11th July – 2nd August, 2014. Four subsoilers which were designed and fabricated using locally sourced and cost-effective materials were tested simultaneously on the soil bin. Four subsoilers constitute the treatments for the experiment. Each subsoiler was mounted on the tool bar of the tool carrier during test. The tool carrier was coupled to the tractor via a bracket carrying the load cell.

The experiment was conducted using selected speed 5 km h^{-1} and rake angles of 27° for each of the treatments. Rake angle of 37° was also employed for straight shank subsoiler. The treatments included:

1. Straight shank subsoiler   -   SSS
2. Straight shank subsoiler at 37° rake angle -   SSS37
3. Semi-Parabolic subsoiler   -   SPS
4. Parabolic C-shank subsoiler   -   CSS
5. Winged Subsoiler   -   WSB

2.8   Measurement of soil disturbance

A calibrated soil profilometer of height and width, 80 and 75 cm was employed in the estimation of area of soil disturbance by the subsoilers. To measure the area of soil disturbed and soil profile produced by the movement of each of the subsoilers, the soil that was loosened or disturbed was removed by hand. Care was taken to ensure that only soil loosened by tillage was removed (Raper, 2002; Kumar and Thakur, 2005; Raper, 2007; Solhjou et al., 2013). The profilometer was placed across the area that was subsoiled and the horizontal rod holding the vertical sliding aluminium rods was removed. Additionally, the vertical rods were slid down and rested according to the geometry of the soil disturbance.

A marker was then used to trace the tips of the rods accordingly on the graph paper. The exact soil profile was estimated by joining these points. The area on the graph which represented the area of soil disrupted was estimated. Also, on the paper the depth and width of disturbance were estimated. This was repeated three times for each of the subsoilers and depths that were considered. Then, the mean values were recorded (see Figure 6(e)).

(a) Experimental layout of the soil bin   (b) Tool Carrier hitched to the tractor   (c) Re-compacting the soil bin with the tractor   (d) Measuring soil disturbance with profilometer

Figure 6   Showing equipment on the experimental site

2.9   Measurement of draughts of subsoilers

The instrumentation assembly was used in measuring the draught of each of the subsoilers at each depth of operation. The load cell was attached to the tool carrier load cell brackets using a screw bolt. The other end of the load cell was also screwed with a bolt firmly and then hitched to the tractor drawbar. The load cell cable was then extended to the instrumentation box attached to the left-hand side of the tractor. This box housed the instrumentation amplifier (print circuit board), which was connected to the load cell, data logger, and the 9 V dry cell batteries. The data logger was also connected to the laptop for the monitoring and downloading of the acquired data, which based on the existing work by Ale et al. (2013) and Ademosun *et al.* (2014).

2.10   Data analysis

Data collected were analyzed using IBM statistical package for social sciences (SPSS) version 21 and Microsoft Excel 2010 to establish relevant relationships between subsoiler draughts and tillage parameters in the form of correlation, regression models and graphs.

3   Results and discussion

3.1   Cone index and moisture content of soil bin before compaction, after compaction and after subsoiling

The initial average cone index values taken at various points on the soil bin showed that cone index at the depth of 0-20 cm was between 0.18-0.44 MPa. While the cone index at the depth of 21-30 cm was at the range of 0.5-1.35 MPa. In another development, the cone index at the depth of 31-50 cm for the points under consideration was between 0.9-1.7 MPa. Thus, the cone index at random points on the soil bin at the three levels of depth were increased to 2.0 MPa and above due to the tractor-induced compaction. The high cone index values

of the soil bin were reduced considerably as a result of subsoiling. Thus, the artificial hard pan created was broken, and the cone index at the three levels of depth was reduced to a range of 0.10-0.60 MPa. This corroborates the findings of Raper (2007) where the cone index and bulk density of soil were reduced after subsoiling.

The range of moisture content at the three levels of depth for different location on the soil bin before compaction, after compaction and after subsoiling revealed a significant difference between them. Thus, the moisture contents at the levels of depth under consideration were observed to be between 8%-19% before compaction, 10%-17% after compaction and 9%-16% after subsoiling. This showed that compaction and subsoiling had significant effects on the range of soil moisture at different depths.

The soil bin textural class was sandy clay (49% sand, 47% clay, and 14% silt), with average porosity of 26%.

3.2 Draught, soil disturbance, specific draughts and power requirement of subsoilers

3.2.1 Draught of subsoilers

Results of the data obtained from testing of subsoilers are displayed in Figure 7-10. Figure 7 shows the relationship between draughts of subsoilers operating at different depths. The use of CSS gave the lowest draught, followed by the SPS, SSS and WSB. The SSS37 working at an increased rake angle of 37° exerted the highest draught. Thus, at operating depth of 20 cm, CSS exerted an average draught of 1,478.50 N, followed by SPS with 2,073.04 N. At this depth of operation, the SSS, WSB and SSS37 had 3,382.83, 3,718.42 and 3,811.60 N respectively.
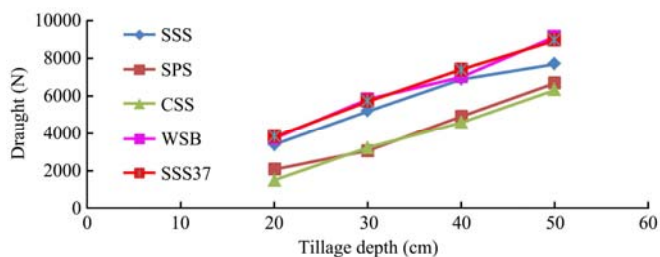

Figure 7   Draught of subsoiler shanks at different depths

On the other hand, at 40 cm working depth, the CSS, SPS, SSS, WSB and SSS37 had draughts of 4581.02, 4905.09, 6874.48, 7003.40 and 7385.28 N respectively. Whereas at 50 cm operating depth, CSS had the lowest

draught of 6,319.90 N and WSB had the highest draught of 9,121.30 N. Thus, the CSS showed signs of bending as the operating depth increased from 30 cm to 40 and 50 cm. This revealed the handicap nature of CSS at high depth of operation due to the surcharge or vertical pressure on the soil, which resulted in the increase of soil failure force. This corroborates the findings of Upadhyaya et al. (1984) and also in accordance with the report of Kumar and Thakur (2005).

The performance of subsoilers in terms of decrease in draught showed that the SPS and CSS had a decrease of 1309.79 N (39%) and 1904.33 N (56%) respectively compared to SSS at working depth of 20 cm. Thus, the decrease in draught was observed for all the working depths. At 40 cm working depth, the decrease in draught for both subsoilers (SPS and CSS) compared with the SSS were 1969.38 N (29%) and 2293.46 N (33%) respectively.

On the other hand, the WSB and SSS37 had an increase in draught of 335.59 N (10%) and 428.77 N (13%) respectively at working depth of 20 cm compared to SSS. While at 50 cm working depth the WSB and the SSS37 had increased draught of 1437.10 N (19%) and 1262.64 N (16%) compared to SSS respectively. Thus, in all the working depths, both subsoilers had varying increase in draught compared to the SSS.

3.2.2 Soil disturbance of subsoilers

Soil loosening abilities of the different subsoilers working at various depths are shown in Figure 8. As demonstrated in the figure, SSS37 showed the highest soil loosening ability at all the depths followed by WSB, SPS, SSS and CSS respectively. Thus, at 20 cm working depth, SSS had an estimated area of soil disturbance of 0.0325 m^2. While the SPS, CSS, WSB and SSS37 had 0.0342, 0.0312, 0.0453 and 0.0561 m^2 respectively. On the other hand, at 50 cm highest working depth, SSS had 0.0451 followed by SPS with 0.0487, while CSS, WSB and SSS37 had 0.0403, 0.0683 and 0.1061 m^2 respectively.

The large area of soil loosened by the SSS37 compared to SSS and other subsoilers revealed the importance of increased rake angle on subsoilers. Although this may call for more draught and energy usage by the prime mover. Thus, the percentage increase in soil disturbance by SPS over SSS for 20, 30, 40 and

50 cm working depths were respectively 5%, 5%, 6% and 8%. While the percentage increase in soil disturbance of WSB over SSS were 39%, 36%, 36% and 51% at working depths of 20, 30, 40 and 50 cm respectively. Whereas the SSS37 had percentage increase of 72%, 103%, 135% and 135% over SSS at depths of 20, 30, 40 and 50 cm respectively.
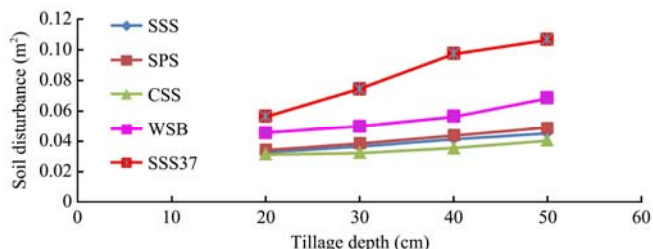

Figure 8   Estimated soil disturbance by subsoilers operating at different depths

3.2.3   Specific draught of subsoilers

Figure 9 shows the specific draughts of the different subsoilers operated at various depths. The figure clearly revealed that the specific draughts of SSS was highest at all depths of operation. Thus at 20, 40 and 50 cm depths of operation, the specific draughts of SSS were 104,087.20, 166,452.39, and 170,381.61 N m^{-2} respectively. On the other hand, the SSS37 had the lowest specific draughts at 30, 40 and 50 cm depths of operation with 76,751.42, 75,980.33 and 84,324.72 N m^{-2} respectively. Whereas the specific draughts of WSB were higher than that of SPS and CSS at operating depths of 20 and 30 cm, but reduced lower than them at increased depths of 40 and 50 cm as depicted on the figure.
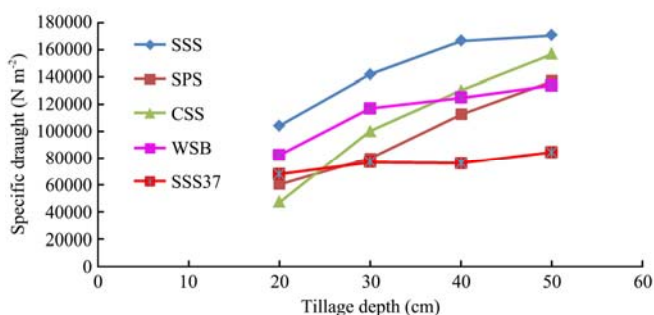

Figure 9   Specific draught of subsoiler shanks at different depths

It should be noted here that at depths lower than 30 cm, the performance in terms of specific draughts of SSS, SPS, CSS WSB and SSS37 were not found to be at par as reported by Di Prinzio et al. (1997) and Kumar and Thakur (2005). This may be due to the fact that the soil was compacted from the top (zero level) to high cone

index (≥2.0 MPa), this condition was different from that of the authors who operated on soils having hard pans at depth of 20 cm and above.

Comparing the subsoilers in terms of percentage reduction in specific draughts, the SPS and CSS had percentage reduction in specific draughts by 42% and 38% (43,471.79 N) and 56,699.35 N) respectively compared to SSS at depth of 20 cm. While at depth of 50 cm, they had reduction in specific draught by 20% and 8% (33,379.72 and 13,560.09 N m^{-2}) respectively. In another development, the WSB and SSS37 had reduction in specific draughts compared with SSS at 20 cm working depth by 21% and 35% (22,002.86 and 36,144.16 N m^{-2}) respectively. While at 40 cm operating depth, WSB and SSS37 had specific draught reduction compared with SSS by 25% and 54% (41,836.64 and 90,472.06 N m^{-2}) respectively. Thus, the SSS37 had the highest specific draught reduction followed by SPS and CSS.

3.2.4   Power requirements of the subsoilers

Power requirements for the operation of the different subsoilers at different depths were calculated from the logged draughts using the equation by Agbetoye (2000):

$$P = (D \times S \times W) \tag{1}$$

where, P = power requirements; D = draught; S = Speed of operation; W = width of disturbance.

Figure 10 shows the power requirements of different subsoilers operated at different depths. WSB had the highest power requirement followed by straight shank subsoiler at 37° rake angle (SSS37), both had 34.09 and 31.20 kW at 50 cm depth respectively. Thus at 20 cm depth of operation WSB and SSS37 subsoilers had 13.95 and 14.29 kW respectively. CSS had the lowest power requirement followed by SPS with 5.55 and 7.76 kW respectively.
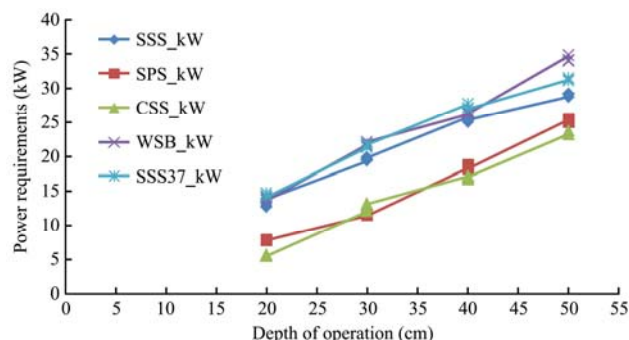

Figure 10   Power requirements for different subsoilers at different depths of operation

3.3 Correlation of draught of subsoilers with depth and soil properties

Draughts of all the subsoilers had high positive correlation with depth, CI, and BD and negative correlation with soil moisture and porosity. Draught of straight shank subsoiler (D_{SSS}) had correlation coefficients of 0.987, 0.995 and 0.983 with depth of operation, cone index (CI) and bulk density (BD) respectively. But negatively correlated with MC and PR with values of −0.332 and −0.954 respectively. On the other hand, draughts of semi-parabolic subsoiler (D_{SPS}) had correlation coefficients of 0.992, 0.957 and 0.997 with depth of operation, cone index, and bulk density respectively; and negative correlation coefficient values of −0.555 and −0.993 with soil moisture and porosity respectively.

In another development, draughts of parabolic 'C' shank subsoilers (D_{CSS}) correlation values of 0.999, 0.987 and 0.991 with depth of operation, cone index and bulk density respectively; but with values of −0.432 and −0.991 with soil moisture and porosity respectively. Draughts of winged subsoiler (D_{WSB}) had correlation coefficients of 0.995, 0.984 and 0.982, −0.419 and −0.991 with depth of operation, cone index, bulk density soil moisture and porosity respectively. While draughts of straight shank subsoiler at rake angle of 37° (D_{SSS37}) had correlation values of 0.999, 0.992, 0.993, −0.409 and −0.983 with depth of operation, cone index, bulk density soil moisture and porosity respectively.

3.4 Regression of draughts of subsoilers with depth and soil properties

Draughts (kN) of the different subsoilers that were logged and downloaded during subsoiling operations were regressed with depth of operation (DP), cone index (CI), bulk density (BD), soil moisture (MC) and soil porosity (PR) to obtain regression equations.

$$D_{SSS} = -0.720 + 0.140DP + 0.506CI - 0.652BD + 3.838MC + 5.869PR \qquad (2)$$

$$D_{SPS} = -0.313 + 0.100DP + 0.154CI + 1.925BD - 9.674\,MC - 11.040PR \qquad (3)$$

$$D_{CSS} = -1.060 + 0.279DP - 1.958CI - 1.066BD + 9.604MC + 10.054PR \qquad (4)$$

$$D_{WSB} = 2.875 + 0.279DP - 1.422CI - 2.015BD + 7.936MC + 2.504PR \qquad (5)$$

$$D_{SSS37} = 0.704 + 0.126DP + 1.049CI - 1.323BD + 4.363MC - 1.785PR \qquad (6)$$

Equation (2) represents the regression model for draught of straight shank subsoiler (D_{SSS}). The equation had $R^2 = 0.992$ and std. error of 0.200. On the other hand, Equation 3 represents the regression model for draught of semi parabolic subsoiler (D_{SPS}) with R^2 value of 0.999 and std. of 0.084. Additionally, Equation (4) shows the regression equation for parabolic 'C' shank subsoiler (D_{CSS}) with R^2 of 0.998 and std. error of 0.115. In another development, the regression equation for draught of winged subsoiler (D_{WSB}) in Equation (5) had an R^2 value of 0.993 with std. of 0.217. While the regression equation for straight shank subsoiler at 37° rake angle (D_{SSS37}) is shown in Equation (6). This equation had a R^2 value of 0.994 and std. of 0.174. Thus, the validation graphs for the above regression equations showed linear relationship between the observed and predicted values of draught for the subsoilers under consideration.

4 Conclusions and recommendations

4.1 Conclusions

The following conclusion can be drawn from this research work:

1. Four types of instrumented subsoiler shanks were designed and their performance were evaluated.

2. Draught requirements of the subsoilers were: parabolic C-shank subsoiler (CSS) with 4.58 kN followed by semi-parabolic subsoiler (SPS) with draught of 4.91 kN at depth of 40 cm. At this working depth, the SSS, WSB and SSS37 had draught of 6.87, 7.00 and 7.39 kN respectively.

3. WSB had the highest power requirement followed by straight shank subsoiler at 37° rake angle (SSS37), which both had 34.09 and 31.20 kW at 50 cm depth respectively. At 20 cm depth of operation, WSB and SSS37 subsoilers had 13.95 and 14.29 kW respectively. CSS had the lowest power requirement followed by SPS with 5.55 and 7.76 kW respectively.

4. At 37° rake angle of straight shank subsoiler, SSS37 showed the highest soil loosening ability at all the depths followed by WSB, SPS, SSS and CSS respectively. Thus, at 50 cm highest working depth, SSS had 0.0451 followed by SPS with 0.0487 while CSS, WSB and

SSS37 had 0.0403, 0.0683 and 0.1061 m^2 respectively.

5. Draught of subsoilers had high positive correlation with depth, CI and BD, and negative correlation with MC and PR.

6. Regression equation for draughts of each of the subsoilers showed high coefficient of linearity between the observed and predicted values.

4.2   Recommendations

It is recommended that farmers should carry out soil tests on their agricultural land before subsequent cultivation to know the state of the soil. Farmers are advised to carry out subsoiling of their agricultural land once every 3-5 years to alleviate soil compaction. This will enhance pulverisation and aeration of soil for easy water infiltration, root development, growth and yield of crops.

Acknowledgements

References

Aase, J. K., D. I. Bjomeberg, and R. E. Sojka. 2001. Zone-subsoiling relationships to bulk density and cone index on a furrow-irrigated soil. *Transactions of ASAE*, 44(3): 577–583.

Atwell, B. J. 1993. Response of roots to mechanical impedance. *Environmental and Experimental Botany*, 33(93): 27–40.

Abu-Hamdeh, N. H. 2003. Compaction and subsoiling effects on corn growth and soil bulk density. *Soil Science Society of America Journal*, 67(4): 1213–1219.

Ademosun, O. C. 2014. Soil tillage dynamics in nigeria: potentials prospects and challenges. proceedings of nigerian branch of international soil tillage research organisation. In *Proceedings of Nigerian Branch of International Soil Tillage Research Organisation*, 26-31. Akure, 3-6 November, 2014.

Agbetoye, L. A. S. 2000. The design and operation for a model cocoyam harvester. *Journal of Science and Technology,* 9(1): 147–151.

Aikins, S. H. M., and J. Kilgour. 2007. Performance evaluation of an ox-drawn ridging plough in a soil bin. *Journal of Science and Technology*, 27(2): 1–9.

Ale, M. O., O. C. Ademosun, S. I. Manuwa, L. A. S. Agbetoye, A. Adesina, and T. Ewetumo. 2013. Assembly and performance evaluation of the instrumentation system of a soil bin for tillage study. In *Proceedings of The Nigerian Institution of Agricultural Engineers*, pages 84–91, Uyo, October 21-24, 2013.

Amauri, N. B., F. C. Jasse, A. P. Maria, F. O. Silva, L. S. Eurica, L. S. Cristian, and P. S. Alvaro. 2008. Traffic soil compaction of oxisol related to soybean development and yield. *Journal of Agricola Science (Piracicaba, Brazil)*, 64(6): 608–615.

Ashrafizadeh, S. R., and R. L. Kushwaha. 2003. Soil failure model in front of a tillage tool action- a review. *The Canadian Society for Engineering in Agricultural, Food and Biological Systems, CSAE*, 2003(03-210): 1–28.

Bandalan, E. P., V. M. Salokhe, C. P. Gupta, and T. Niyamapa. 1999. Performance of an oscillating subsoiler in breaking a hardpan. *Journal of Terramechanics*: 36(1999): 117–125.

Becerra, A. T., G. F. Botta, X. L. Bravo, M. Tourn, F. B. Melcon, J. Vazquez, D. Rivero, P. Linares, and G. Nardon. 2010. Soil compaction distribution under tractor traffic in almond (*Prunus amigdalus* L.) orchard in Almeria Espana. *Soil and Tillage Research*, 107(1): 49–56.

Becerra, A. T., M. Tourn, G. F. Botta, and X. L. Bravo. 2011. Effects of different tillage regimes on soil compaction, maize (Zea mays L.) seedling emergence and yields in eastern Argentina Pampas region. *Soil and Tillage Research*, 107(1): 184–190.

Bengough, A. G. 1991. The penetrometer in relation to mechanical resistance. In *Soil Analysis. Physical Method,* eds. K. A. Smith, and C. E. Mullins, 431–446. New York: Marcel Dekker.

Blake, G. R., and K. H. Hartge. 1986. Bulk density. In *Methods of Soil Analysis (2nd Ed),* ed. A. Klute, part1 No.9, 363–375. Madison, Wisconsin: ASA-SSSA.

Borghei, A. M., J. Taghinejad, S. Minaei, M. Karimi, and M. G. Varnamkhasti. 2008. Effect of subsoiling on soil bulk density, penetration resistance and cotton yield in northwest of Iran. *International Journal of Agriculture and Biology*, 10(2): 120–123.

Celik, A., and R. L. Raper. 2012. Design and evaluation of ground-driven rotary subsoilers. *Soil and Tillage Research*, 124: 203–210.

Chen, G., and R. R. Weil. 2011. Root growth and yield of maize as affected by soil compaction and cover crops. *Soil and Tillage Research,* 117: 17–27.

Chen, Y., N. B. McLaughlin, and S. Tessier. 2007. Double extended octagonal ring (DEOR) drawbar dynamometer. *Soil and Tillage Research*, 93: 462–471.

Clark, R. L., D. E. Kissel, F. Chen, and W. Adkins. 2000. Mapping soil hardpans with the penetrometer and soil electrical conductivity. ASAE Paper No. 00-1042. St. Joseph, Mich.: ASAE.]

D'Haene, K., J. Vermang, W. M. Cornelis, B. L. M. Leroy, W. Schiettecatte, S. De Neve, D. Gabriels, and G. Hofman. 2008.

Reduced tillage effects on physical properties of silt loam soils growing root crops. *Soil and Tillage Research*, 99: 279–290.

Di Prinzio, L. A. P., V. C. D. Ayala, T. J. C. Magdalena, and L. A. P. Di Prinzio. 1997. Energetic test of different subsoiling Techniques and its effects upon the soil bulk density. *Agro-Ciencia (Chile)*, 13(1): 61–67.

Godwin, R. J. 2007. A review of the effect of implement geometry on soil failure and implement forces. *Soil and Tillage Research,* 97(2007), 331–340.

Gregory, P. J. 1994. Root growth and activity. In *Physiology and Determination of Crop Yield,* eds K. J. Boote, J. M. Bennett, T. R. Sinclair, and G. M. Paulsen, 65–93. Madison: ASA-CSSA-SSSA.

Grzesiak, M. T. 2009. Impact of soil compaction on root architecture, leaf water status, gas exchange and growth of maize and triticale seedlings. *Plant Root,* vol. 3: 10–16.

Isaac, N. E., R. K. Talor, S. A. Staggenborg, M. D. Schrock, and D. F. Leikam. 2002. Using cone index data to explain yield variation within a field. *CIGR Journal*, Written for presentation at the 2002 ASAE Annual International Meeting Hyatt Regency Chicago, Chicago, Illinois, USA, July 29 – 31, 2002.

Juliano, C. C., and C. A. Rosolem. 2010. Soybean root growth and yield in rotation with cover crops under chiseling and no-till. *European Journal of Agronomy*, 33(3): 242–249.

Kees, G. 2008. Using Subsoiling to Reduce Soil Compaction. Technology & Development Program 0834–2828–MTDC. Missoula, MT: U.S. Department of Agriculture, Forest Service, Missoula Technology and Development Center.

Kulkarni, S. S., S. G. Bajwa, and G. Huitink. 2010. Investigation of the effects of soil compaction in cotton. *Transactions of the ASABE*, 53(3): 667–674.

Kumar, A., and T. C. Thakur. 2005. An investigation into comparative test of conventional and winged subsoilers. ASAE Paper No. 051061. St. Joseph, Mich.: ASAE.

Manuwa, S. I. 2002. Development of an equipment for soil tillage dynamics and evaluation of tillage parameters. Ph.D. diss., Department of Agricultural Engineering, Federal University of Technology, Akure, Nigeria.

Manor, G., and R. L. Clark. 2001. Development of an instrumented subsoiler to map soil hard-pans and real-time control of subsoiler depth. ASAE Paper No. 011022. St. Joseph, Mich.: ASAE.

Mason, E. G., A. W. J. Cullen, and W, C, Rijkse. 1988. Growth of two pinus radiate stock types on ripped and ripped/bedded plots at karioi forest. *New Zealand Journal of Forestry Science*, 18(3): 287–296.

Mollazade, K., A. Jafari, and E. Ebrahimi. 2010. Application of dynamical analysis to choose best subsoiler's shape using ANSYS. *New York Science Journal*, 3(3): 93–100.

Otto, R., A. P. Silva, H. C. J. Franco, E. C. A. Oliveira, and P. C. O.

Trivelin. 2011. high soil penetration resistance reduces sugarcane root system development. *Journal of Soil and Tillage Research*, 117: 201–210.

Radcliffe, D. E., G. Manor, G. W. Langdale, R. L. Clark, and R. R. Bruce. 1989. Effect of traffic and in-row chiseling on mechanical impedance. *Soil Science Society of America Journal*, 53(4): 1197–1201.

Raper, R. L., D. W. Reeves, and E. C. Burt. 1998. Using in-row subsoiling to minimize soil compaction caused by traffic. *Journal of Cotton Science*, 2(3): 130–135.

Raper, R. L. 2002. Force requirements and soil disruption of straight and bentleg subsoilers for conservation tillage systems. ASAE Paper No. 021139. St. Joseph, Mich.: ASAE.

Raper, R. L. 2007. In-row subsoilers that reduce soil compaction and residue disturbance. *Transaction of the American Society of Agricultural and Biological Engineers*, 23(3): 253–258.

Raper, R. L., and A. K. Sharma. 2004. Soil Moisture effects on energy requirements and soil disruption of subsoiling of coastal plain soil. *Transaction of the American Society of Agricultural Engineers,* 47(6): 1899–1905.

Sakai, K., S. I. Hata, M. Takai, and S. Nambu. 1993. Design parameters of four-shank vibrating subsoiler. *Transaction of the American Society of Agricultural Engineers,* 36(1): 23–26.

Sakai, K., H. Terau, and K. Matsui. 1983. The study on vibratory soil cutting by a vibratory subsoiler (Part 1.). The optima cutting directional angle. *Journal of Japanese Society of Agricultural Machinery*, 45(1): 55–62.

Soltanabadi, M. H., L. M. Miranzadeh, L. M. Karimi, M. G. Varnamkhasti, and A. Hemmat. 2008. Effect of subsoiling on soil physical properties and sun flower yield under conditions of conventional tillage. *International Agrophysics*, 22(4): 313–317.

Solhjou, A., J. M. A. Desbiolles, and J. M. Fielke. 2013. Soil translocation by narrow openers with various blade face geometries. *Biosystems Engineering*, 114(2013): 259–266.

Tardieu, F. 1994. Growth and functioning of roots and of root systems subjected to soil compaction. Towards a system with multiple signalling. *Soil Tillage Research*, 30(2-4): 217–243.

Taylor, J. H. 1990. Soil compaction research in the eighties: an international overview. ASAE Paper No. 90-1072. St. Joseph, Mich.: ASAE.

Weber, R., and A. Biskupski. 2008. Effect of penetration resistance, bulk density and moisture content of soil on selected yield components of winter triticle in relation to method of cultivation. *International Agrophysics*, 22(2): 171–177.

Wells, L. G., T. S. Stombaugh, and S. A. Shearer. 2005. Crop yield response to precision deep tillage. *Transactions of the ASAE,* 48(3): 895–901.

Williams, J. D., S. B. Wuest, W. F. Schillinger, and H. T. Gollany. 2006. Rotary subsoiling of newly planted wheat fields to improve infiltration in frozen soil. *Soil and Tillage Research,* 86: 141–151.